

Online Research @ Cardiff

This is an Open Access document downloaded from ORCA, Cardiff University's institutional repository: <http://orca.cf.ac.uk/107970/>

This is the author's version of a work that was submitted to / accepted for publication.

Citation for final published version:

Tardugno, Roberta, Giancotti, Gilda, De Burghgraeve, Tine, Delang, Leen, Neyts, Johan, Leysen, Pieter, Brancale, Andrea and Bassetto, Marcella 2018. Design, synthesis and evaluation against Chikungunya virus of novel small-molecule antiviral agents. *Bioorganic and Medicinal Chemistry* 26 (4) , pp. 869-874. 10.1016/j.bmc.2018.01.002 file

Publishers page: <http://dx.doi.org/10.1016/j.bmc.2018.01.002>
<<http://dx.doi.org/10.1016/j.bmc.2018.01.002>>

Please note:

Changes made as a result of publishing processes such as copy-editing, formatting and page numbers may not be reflected in this version. For the definitive version of this publication, please refer to the published source. You are advised to consult the publisher's version if you wish to cite this paper.

This version is being made available in accordance with publisher policies. See <http://orca.cf.ac.uk/policies.html> for usage policies. Copyright and moral rights for publications made available in ORCA are retained by the copyright holders.



Design, synthesis and evaluation against Chikungunya virus of novel small-molecule antiviral agents

Roberta Tardugno^a, Gilda Giancotti^a, Tine De Burghgraeve^b, Leen Delang^b, Johan Neyts^b, Pieter Leyssen^b, Andrea Brancale^a, Marcella Bassetto^{a1}

^aCardiff School of Pharmacy and Pharmaceutical Sciences, Cardiff, King Edward VII Avenue, Cardiff CF103NB, UK

^bRega Institute for Medical Research, University of Leuven, Belgium

Abstract

Chikungunya virus is a re-emerging arbovirus transmitted to humans by mosquitoes, responsible for an acute flu-like illness associated with debilitating arthralgia, which can persist for several months or become chronic. In recent years, this viral infection has spread worldwide with a previously unknown virulence. To date, no specific antiviral treatments nor vaccines are available against this important pathogen. Starting from the structures of two antiviral hits previously identified in our research group with *in silico* techniques, this work describes the design and preparation of 31 novel structural analogues, with which different pharmacophoric features of the two hits have been explored and correlated with the inhibition of Chikungunya virus replication in cells. Structure-activity relationships were elucidated for the original scaffolds, and different novel antiviral compounds with EC₅₀ values in the low micromolar range were identified. This work provides the foundation for further investigation of these promising novel structures as antiviral agents against Chikungunya virus.

1. Introduction

Chikungunya virus (CHIKV) is an Arbovirus that belongs to the Alphavirus genus of the Togaviridae family. Transmitted to humans by mosquito *Aedes Aegypti*, it is associated with an acute pathology characterised by fever, rash and arthralgia. The last condition is often severe and may persist for several months or become chronic in the 10% of infected individuals.¹ CHIKV infection was first described in Tanzania in 1952 and since 2005 it re-emerged with a previously unknown virulence in Africa, Indian Ocean, India and South-East Asia, reaching Europe and the US.²⁻³ The ability to adapt to a new vector, the mosquito *Aedes Albopictus*, has contributed to the worldwide spread of the infection.⁴ Clinically approved compounds such as chloroquine, alpha-interferon and ribavirin, even if showing some antiviral effect *in vitro*, demonstrated poor *in vivo* activity against CHIKV infection and, to date, no specific treatment is available, nor a vaccine is approved: the therapy is still limited to supportive treatment of the symptoms.⁵⁻⁶ Research interest on CHIKV has been rapidly increasing in the last few years. However, to date, only few selective anti-CHIKV agents have been reported, and none of them has reached the clinical evaluation stage.⁷

As part of an ongoing project aiming to identify novel inhibitors of Chikungunya virus replication, the structures of our previous hits **1** and **2** (**Figure 1**), identified as inhibitors of the CHIKV life cycle

¹ Corresponding author

E-mail address: bassettom@cardiff.ac.uk (Dr. M. Bassetto)

following a docking-based virtual screening analysis of commercial compounds on the structure of the viral nsP2 protease,⁸ have been modified to gain insights into the antiviral structure-activity relationships associated with this molecular scaffold. These novel structural modifications led to a deeper understanding of the pharmacophoric features required for antiviral activity and to the identification of novel anti-CHIKV agents with antiviral EC₅₀ values in the low micromolar range and good selectivity indexes.

2. Results and discussion

2.1 Rational design of novel analogues

The scaffold of hits **1** and **2** is characterised by the presence of two differently substituted phenyl rings, ring A and ring B, a hydrazone group directly attached to ring B, and an aliphatic spacer (a cyclopropyl group in the trans configuration or a trans double bond) connecting ring A with the central hydrazone function. In order to further explore the antiviral structure-activity relationships associated with these agents, and taking into account our previously reported preliminary explorations of their structures,⁸ a series of 31 novel molecular analogues was designed and synthesised. As summarised in **Figure 1**, several new modifications to the original structures were carried out in order to: 1. explore different aromatic substituents on the two phenyl rings, while maintaining a central linker characterised by a cyclopropyl group in the trans configuration or a trans double bond linked to a hydrazone feature; 2. replace the original hydrazone with a more stable amide function; 3. investigate the role of the rigidity of the central linker by reducing the trans-double bond to an ethyl group.

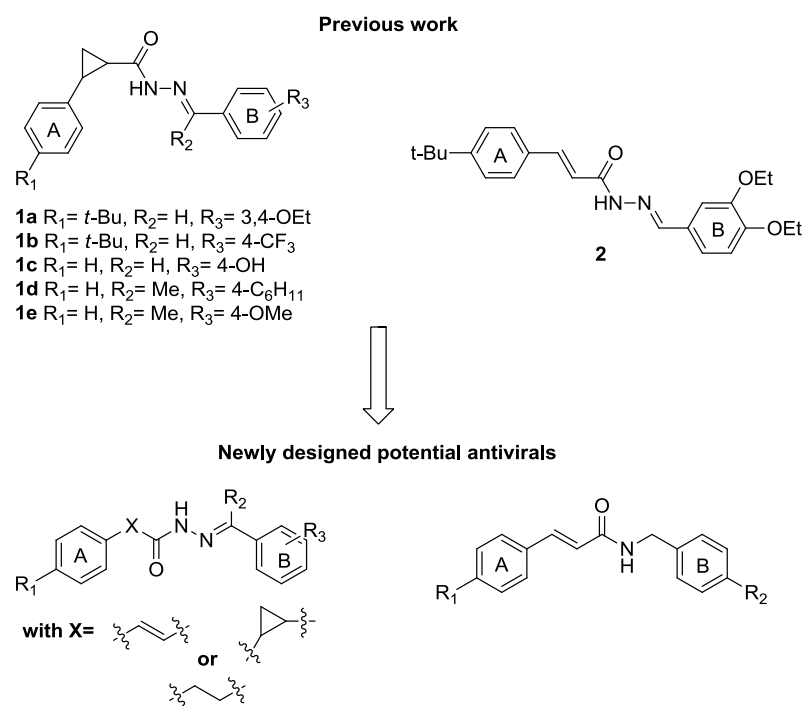
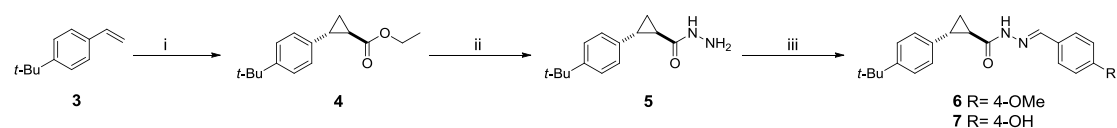


Figure 1. Structure of our previous antiviral hits and their proposed modifications.

With the aim to take into account and to further confirm our previously reported structural considerations,⁸ the novel analogues were designed to either maintain a hydrophobic substituent (*tert*-butyl or methyl) in the *para* position of aromatic ring A, or to remove completely this substituent, in order to assess its essential role for antiviral activity. The nature and presence of the two original ethoxy groups in aromatic ring B was also extensively explored to understand their role in the inhibition of the viral replication. Due to the easier purification associated with the presence of a trans double bond replacing the trans-cyclopropylic ring of the original hit, and to the fact that **2** is not associated with any cytotoxic effect *in vitro*,⁸ most of the planned modifications on the two aromatic systems were carried out on the trans-ethylidene scaffold of **2**. As a first attempt to improve the stability of **2**, which is not predicted to be highly stable in aqueous conditions due to the presence of a hydrazone function, a small series of novel analogues was envisaged to replace this group with a more stable amide bond. In the case of this last modification, in order to partially compensate for the reduced overall length of the molecule, which appears to be detrimental for antiviral activity according to our previous preliminary SAR data obtained for the original scaffold **1**,⁸ the insertion of an amide linker was only attempted with a bi-phenyl system replacing ring B, or with a *para*-trifluoromethyl substituent on aromatic ring B.

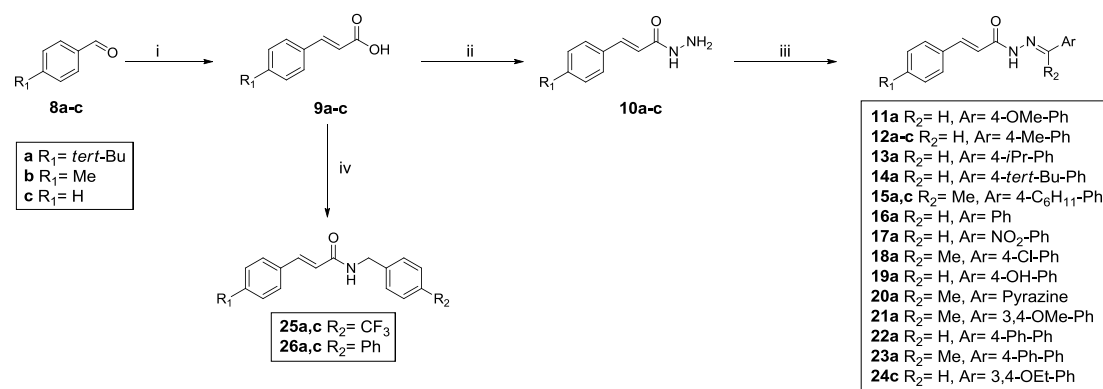
2.2 Chemistry

All target compounds were synthesised according to an optimised two to four-step synthetic pathway, as shown in **Schemes 1-3**.



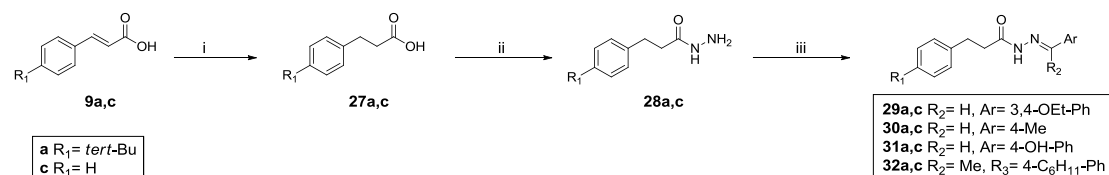
Scheme 1: Reagents and conditions: i. ethyldiazoacetate, 125 °C, 4 h, r.t., o.n. (45%); hydrazine monohydrate, EtOH, reflux, o.n. (85%); differently substituted benzaldehyde, EtOH, reflux, 24 h (54-76%).

Following our previously reported procedure,⁸ a small series of novel cyclopropyl derivatives was prepared by reaction of 4-*tert*-butyl styrene with ethyldiazoacetate at 125 °C for 4h, followed by stirring at r.t. o.n. In these conditions, a mixture of the two diastereomeric couples of enantiomers at the cyclopropane ring is obtained (*cis* and *trans*), and the desired pure *trans*-substituted intermediate **4** was isolated after chromatographic purification in a mixture of dichloromethane and diethyl ether. Ester **4** was then refluxed in EtOH with an excess of hydrazine monohydrate to yield hydrazide **5**, which was then treated with the appropriate differently substituted benzaldehyde to afford final hydrazones **6** and **7**. These final products were envisaged to further investigate our previous findings suggesting that a hydroxyl group in the *para* position of aromatic ring B is tolerated by its introduction together with the *tert*-butyl substituent in ring A (**7**) and by its alkylation to methyl ether (**6**).



Scheme 2: Reagents and conditions: i. malonic acid, cat. piperidine, pyridine, r.t., 3h (93-98%); ii. (a) oxalyl chloride, Et₂O, r.t., 3 h, (b) hydrazine monohydrate, r.t., 2 h (50-63%); iii. differently substituted benzaldehyde, EtOH, reflux, 24 h (65-77%); iv. differently substituted benzylamine, TBTU, diisopropylethylamine, anhydrous DMF, r.t., o.n. (83-96%).

A series of 17 novel benzylidene-acrylohydrazides was instead prepared to further explore the effect of the aromatic substituents on aromatic rings A and B on the scaffold of **2**. Cinnamic acids **9a-c** were prepared following a Knoevenagel condensation- Doebner modification reaction between aldehydes **8a-c** and malonic acid, in the presence of catalytic amounts of piperidine and refluxing the mixture in pyridine.⁹ Acid intermediates **9a-c** were then converted to the corresponding acyl chlorides using oxalyl chloride,¹⁰ and treated *in situ* with hydrazine monohydrate to give acrylo-hydrazides **10a-c**,¹¹ which were finally reacted with differently substituted benzaldehydes or acetophenones to give target compounds **11-24**.¹² Starting from intermediate acids **9a** and **9c**, a small family of 4 novel acrylamide analogues was obtained following a TBTU-assisted coupling reaction with differently substituted benzylamines in the presence of diisopropylamine.¹³ This last modification was envisaged as a means to replace the hydrazone function on the final products with a more stable amide group. Due to the overall reduced length of the scaffold, and according to some preliminary results obtained for the corresponding amide product with a 3,4-dimethoxy substituent on aromatic ring B,⁸ this structural change from hydrazone to amide was envisaged together with the insertion of a biphenyl system to replace ring B (**26a, c**). **25a** and **25c** were prepared to compare the effect of the second phenyl ring with a smaller hydrophobic group, namely the trifluoromethyl.



Scheme 3: Reagents and conditions: i. H₂, 10% Pd/C, THF, r.t., 4h (93-98%); ii. (a) 1.25 M HCl in MeOH, reflux, o.n., (b) hydrazine monohydrate, EtOH, reflux, o.n. (65-67%); differently substituted benzaldehyde, EtOH, reflux, 24 h (73-95%).

As a first attempt to investigate the role of the rigidity of the original linker (trans-cyclopropylhydrazide or acrylohydrazide), a small family of 8 novel analogues was designed to replace the two rigid systems in the original hits with a reduced ethyl group connecting aromatic ring A with the hydrazide portion of the scaffold. The desired modification was achieved by catalytic hydrogenation of cinnamic acids **9a** and

9c to their unsaturated counterparts **27a** and **27c**, performed under H₂ atmosphere in the presence of 10% Pd/C catalyst.¹⁴ The unsaturated acid intermediates **27a, c** were then converted to their methyl ester counterparts by refluxing in 1.25M HCl in methanol, and subsequently treated with hydrazine monohydrate in boiling EtOH to achieve the desired ester displacement in hydrazides **28a, c**.¹⁵ Final compounds **29-32** were obtained as reported for the other two series of hydrazone compounds, by reacting hydrazides **28a, c** with the appropriately substituted benzaldehyde or acetophenone in refluxing EtOH for 24 hours.

2.3 Antiviral and cytotoxicity studies

All the newly synthesised compounds were evaluated for their potential anti-CHIKV activity in Vero cells, investigating their ability to inhibit the cytopathogenic effect (CPE) induced by the virus, and for their potential cytotoxicity. The known anti-CHIKV agent Chloroquine was included as positive control.¹⁶

Table 1: Antiviral effect of the test compounds on CHIKV replication in Vero cells and cytotoxicity.

Comp.	Scaffold	Chemical Structure			EC ₅₀ (μM) ^{a,d}	EC ₉₀ (μM) ^{b,d}	CC ₅₀ (μM) ^{c,d}	SI ^e
		R ₁ (ring A)	R ₂	Ar (ring B)				
1a^f	a	<i>t</i> -Bu	H	3,4-OEt-Ph	5.0±0.2	6.4±0.5	72±20	14
1b^f	a	<i>t</i> -Bu	H	4-CF ₃ -Ph	14±6	19±10	30±5	2.1
1c^f	a	H	H	4-OH-Ph	6.4±0.1	8.7±0.2	15±1	2.3
1d^f	a	H	Me	4-C ₆ H ₁₁ -Ph	32±1	44±1	101±1	3.1
1e^f	a	H	Me	4-OMe-Ph	5.6±2	12±6	72±2	13
2^f	b	<i>t</i> -Bu	H	3,4-OEt-Ph	3.2±1.8	11±4	101±50	32
6	a	<i>t</i> -Bu	H	4-Me-Ph	6.6	n.d.	n.d.	-
7	a	<i>t</i> -Bu	H	4-OH-Ph	2.7	3.8	n.d.	-
11a	b	<i>t</i> -Bu	H	4-OMe-Ph	5.9±0.8	38.8±16.4	117±23.8	19.8
12a	b	<i>t</i> -Bu	H	4-Me-Ph	5.8±0.9	10±3.4	124±7.1	21.4
12b	b	Me	H	4-Me-Ph	>359	>359	n.d.	-
12c	b	H	H	4-Me-Ph	93.3	>284	84.4±11.5	0.9
13a	b	<i>t</i> -Bu	H	4- <i>i</i> Pr-Ph	2.1±2.4	n.d.	7.4±0.6	3.5
14a	b	<i>t</i> -Bu	H	<i>t</i> -Bu-Ph	>276	>276	n.d.	-
15a	b	<i>t</i> -Bu	Me	4-C ₆ H ₁₁ -Ph	>248	>248	n.d.	-
15c	b	H	Me	4-C ₆ H ₁₁ -Ph	>289	>289	n.d.	-
16a	b	<i>t</i> -Bu	H	Ph	5.8±1.4	87.5±79.1	22.1±6.8	3.8
17a	b	<i>t</i> -Bu	H	4-NO ₂ -Ph	>285	>285	n.d.	-
18a	b	<i>t</i> -Bu	Me	4-Cl-Ph	>282	>282	n.d.	-
19a	b	<i>t</i> -Bu	H	4-OH-Ph	n.d.	n.d.	7.3±1.9	-
20a	b	<i>t</i> -Bu	Me	Pyrazine	103	122±32.1	>310	1.2
21a	b	<i>t</i> -Bu	Me	3,4-OMe-Ph	>263	>263	n.d.	-
22a	b	<i>t</i> -Bu	H	4-Ph-Ph	n.d.	n.d.	20.1±12.6	-
23a	b	<i>t</i> -Bu	Me	4-Ph-Ph	>252	>252	n.d.	-
24b	b	Me	H	3,4-OEt-Ph	113	>284	>284	>2.5
25a	d	<i>t</i> -Bu	CF ₃	-	125±91.1	47.9	115±11	0.9

25c	d	H	CF ₃	-	>246	>246	n.d.	-
26a	d	<i>t</i> -Bu	Ph	-	2.9	>271	4.3±1.1	-
26c	d	H	Ph	-	>319	>319	n.d.	-
29a	c	<i>t</i> -Bu	H	3,4-OEt-Ph	>11	>11	n.d.	-
29c	c	H	H	3,4-OEt-Ph	>294	>294	n.d.	-
30a	c	<i>t</i> -Bu	H	4-Me-Ph	>100	>100	n.d.	-
30c	c	H	H	4-Me-Ph	>375	>375	n.d.	-
31a	c	<i>t</i> -Bu	H	4-OH-Ph	36.4	n.d.	n.d.	-
31c	c	H	H	4-Me-Ph	>373	>373	n.d.	-
32a	c	<i>t</i> -Bu	Me	4-C ₆ H ₁₁ -Ph	>82.4	>82.4	n.d.	-
32c	c	H	H	4-C ₆ H ₁₁ -Ph	>96	>96	n.d.	-
Chloroquine	-	-	-	-	11±7	21±18	89±28	8.1

^a EC₅₀ = 50% effective concentration (concentration at which 50% inhibition of CPE is observed).

^b EC₉₀ = 90% effective concentration (concentration at which 90% inhibition of CPE is observed).

^c CC₅₀ = 50% cytostatic/cytotoxic concentration (concentration at which 50% adverse effect is observed on the host cell).

^d The EC₅₀, EC₉₀ and CC₅₀ values are the mean of at least 3 independent experiments, with standard deviations of ±10% of the value quoted unless otherwise stated (mean value ± standard deviations).

^e SI = the ratio of CC₅₀ to EC₅₀.

^f Biological data as previously reported.⁸

n.d.= value could not be calculated.

Considering together both antiviral activity results and cytotoxicity associated with the novel compounds, the small series of cyclopropyl derivatives **6-7** appears to be correlated with an overall activity retention, confirming what already observed to some extent for the previously reported series of analogues. Alkylation of this hydroxyl group to methoxy is also tolerated, suggesting that the presence and nature of the substituent in ring B is not relevant for the biological potential of the scaffold. In the acrylohydrazone series of structures (**11-24**), most of the antiviral potential appears to be associated with the presence of a *tert*-butyl substituent at the *para* position in aromatic ring A, together with an unsubstituted hydrazone linker and a small hydrophobic group (methyl or methoxy) at the *para* position of aromatic ring B, as indicated by the fact that the best results in terms of antiviral activity and SI index are achieved with **11a** and **12a**. Even though their selectivity index is lower in comparison with **2** (the least toxic compound previously identified), the CC₅₀ values obtained for these two novel structures show a significantly reduced standard deviation in comparison with **2**, allowing a greater confidence in the evaluation of their safety in cells. The antiviral activity of the scaffold seems to be simultaneously influenced by the nature of the two aromatic substituents, as the association of a 4-methyl substituent or of the original 3,4-diethoxy substituent in ring B with a smaller substituent as the 4-methyl group in ring A is associated with loss of antiviral activity (**12b**, **24b**), and the same effect is obtained with an unsubstituted phenyl ring A (**12c**). Surprisingly given the structural features of **2**, increasing the size of the 4-methyl group in **12a** to an isopropyl substituent (**13a**) is related to a significantly increased cytotoxic effect, while a *tert*-butyl group in this position (**14a**) is associated with a complete loss of both antiviral and cytotoxic effect. Trying to investigate the effect of a methyl-substituted hydrazone linker and a 4-cyclohexyl substituent in ring B, previously observed as partially tolerated with **1d**, **15a** and **15c** have been prepared carrying this double modification. The complete loss of activity associated with both these analogues suggests a different trend in antiviral effect associated with the cyclopropyl scaffold of

1a-e and the acrylo structure of **2**. The removal of the substituent in ring B (**16a**) is associated with an increased cytotoxicity, while replacement of the *para* substituent in this ring with a 4-nitro (**17a**) or a 4-chloro (**18a**) moiety led to complete loss of activity. Introduction of a 4-hydroxy group in ring B (**19a**), which was envisaged as a means to increase the polarity and therefore the water solubility of the scaffold, is associated with cytotoxicity, further confirming the different trend for biological effects between the cyclopropylic and acrylo series of compounds. Another attempt to obtain a more polar structure was carried out with the replacement of ring B with a pyrazine group (**20a**), but this modification led to a significant activity reduction. Insertion of an extra phenyl group at the *para* position of ring B in the unsubstituted hydrazone scaffold (**22a**) leads to cytotoxicity, while the same modification on the methyl-hydrazone structure (**23a**) does not show the same cytotoxic effect, but is associated with complete loss of activity. The same effect can be observed for the presence of the substituted methyl-hydrazone linker and a 3,4-methoxy substitution in ring B (**21a**), suggesting that the presence of an unsubstituted hydrazone central linker is essential for antiviral activity retention in the acrylo-hydrazone family of structures. The replacement of the hydrazone group with a more stable and more flexible benzylamide (**25-26**) is associated with either loss of antiviral activity (**25a**, **25c**, **26c**) or with an increased cytotoxicity (**26a**).

Except for **31a**, which seems to partially retain some antiviral effect with an EC₅₀ in the micromolar range, all the remaining unsaturated analogues **29-32** are associated with a complete abolishment of antiviral effect, suggesting that the rigidity of the scaffold and the molecular geometry given by the trans-cyclopropane or trans-double bond are essential for the antiviral effect of these molecules. A general summary of the structure-activity relationships observed for the scaffold of **1** and **2** is depicted in **Figure 3**.

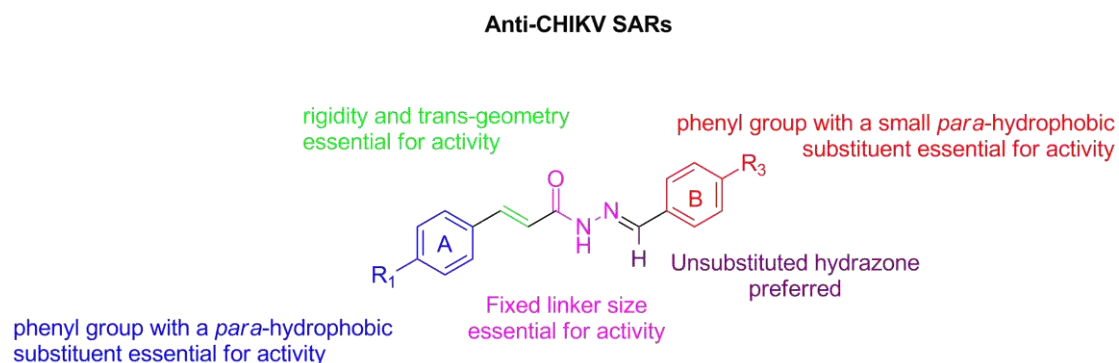


Figure 3. Summary of the antiviral structure-activity relationships obtained with this work for the antiviral scaffold of **1** and **2**.

2.4 Molecular modelling

As briefly explained in the Introduction, the original hit **1** was identified as a selective antiviral agent against CHIKV following a docking-based virtual screening procedure of commercial compounds, with which the structure of the CHIKV nsP2 protease, an essential enzyme for the viral replication, had been chosen as target for the selection of potential inhibitors of the viral replication.⁸ Both hits **1** and **2** are predicted to exert their antiviral activity through the inhibition of this enzyme, by binding to its catalytic pocket. Even though a recently published study suggests that **1** is not a strong inhibitor of CHIKV nsP2 activity *in vitro*,¹⁷ three of our previously reported close analogues of **1** were instead found, in the same

study, to inhibit the proteolytic activity of CHIKV nsP2, along with several novel closely related derivatives of **1**, described in the same work, which all show inhibition of the CHIKV protease activity in the reported enzymatic assay. Due to these indications, the predicted binding to the protease active site was investigated for the novel compounds prepared, with the aim to possibly find a rational explanation for the differences in activity found for the new structures. Glide SP docking algorithm was used for all simulations carried out.¹⁸⁻¹⁹ The predicted binding to the nsP2 protease found for our original hit **2** and representative novel analogues **12a**, **25a** and **29a** is shown in **Figure 4**.

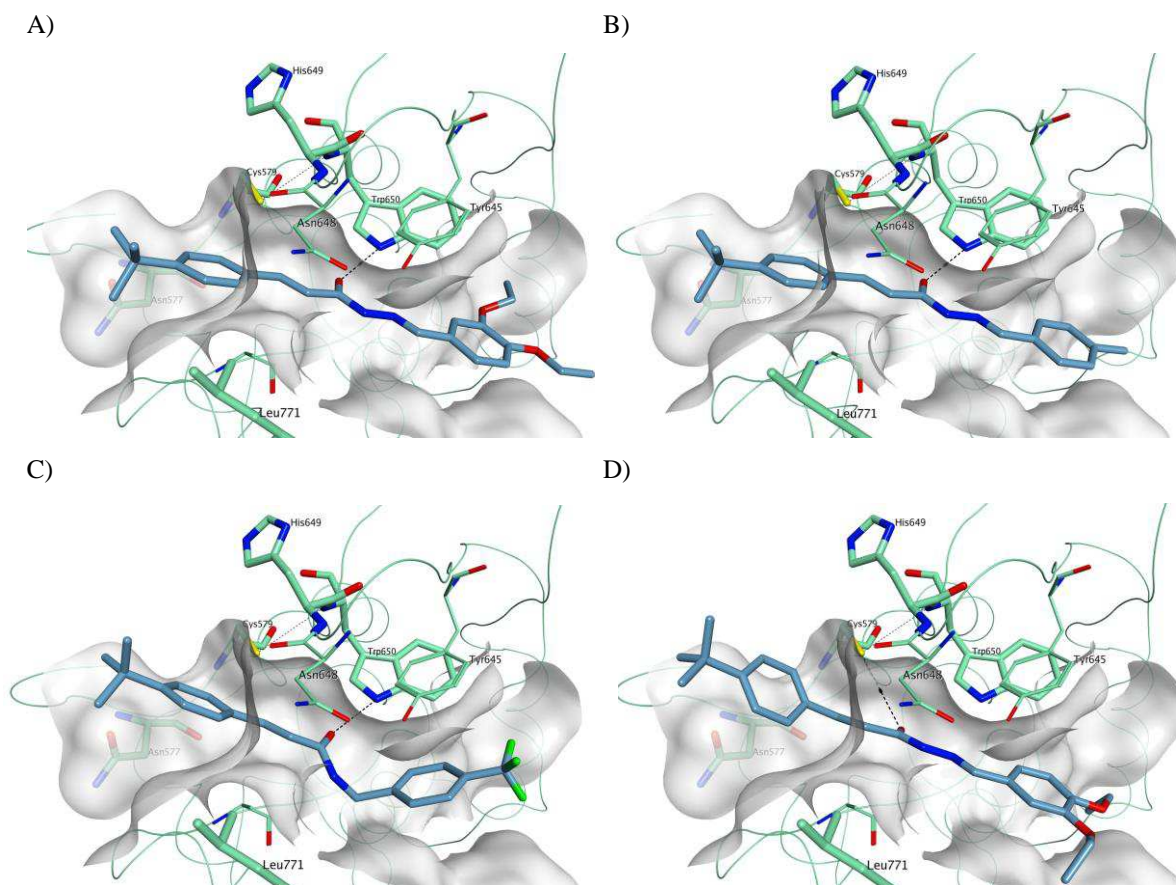


Figure 2. Predicted binding mode of **2** (A), **12a** (B), **25a** (C) and **29a** (D) to the proteolytic site of CHIKV nsP2 (PDB ID 3TRK).

According to our molecular modelling predictions, the hydrazide bond of **2** (**Figure 2A**) fits with high affinity the proteolytic site of the enzyme and is involved, through its carbonyl oxygen, in a direct hydrogen bond with the side chain of Trp650. The two aromatic portions, even though not involved in direct interactions with the surrounding enzyme residues, appear important to anchor the central portion of the molecule in the region defined by the catalytic triad. A very similar binding mode is shared by **12a** (**Figure 2B**), which retains the antiviral effect of **2** and is representative of the two first series of novel compounds prepared, **6**, **7** and **11-24**. Docking results on the CHIKV nsP2 protein catalytic pocket found for all the compounds in these two series (data not shown) do not reveal significant differences in their predicted binding mode to the enzyme active site, possibly indicating that the reason for their marked differences in antiviral activities might be related with cell-penetration factors or with the additional interaction with different viral or host targets. A significant difference in predicted binding is instead

found for **25a**, representative of the small amide series of compounds prepared, for which the loss of activity can be correlated with its increased flexibility, which does not allow an optimal fitting of the protein sub-site surrounding the catalytic residues, and to the overall reduced size of the molecule. The same negative effect associated with the increased flexibility can be speculated for **29a**, where the saturation of the double bond in trans configuration is associated with a different occupation of the target site, as in most of the predicted binding poses found the hydrogen bond with Trp650 is lost in favour of a predicted interaction with Cys579.

3. Conclusions

Starting from the structures of two anti-CHIKV hits previously identified, different series of novel analogues were designed and synthesised to explore the structure-activity relationships associated with these antiviral agents. Different structural elements were identified as essential for antiviral properties, such as the presence of a *tert*-butyl substituent on ring B, an unsubstituted hydrazone linker and the overall length and rigidity of the acrylo-hydrazide scaffold, while the associated antiviral effect was found to follow a different trend for the two original hit scaffolds **1** and **2**. Different novel antiviral agents with anti-CHIKV EC₅₀ values in the low micromolar range and good selectivity indexes were identified, while further structural modifications are the focus of present investigations and will be reported in due course. In particular, present synthetic efforts are directed towards the insertion of the trans-double bond of **2** in a condensed aromatic ring, on the replacement of the central linker with more stable groups while maintaining the overall length of the molecule, and on the inclusion of the central hydrazone group in a third aromatic ring.

Acknowledgements

This research is supported by the Sêr Cymru II programme, which is part-funded by Cardiff University and the European Regional Development Fund through the Welsh Government. L.D. was funded by the Research Foundation of Flanders (FWO). We thank Stijn Delmotte and Tom Bellon for excellent technical assistance.

A. Supplementary data

All experimental procedures and compound characterisation data are reported and described in detail in the Supporting Information.

References

- 1 Ziegler, S.A.; Lu, L.; da Rosa, A.P.; Xiao, S.Y.; Tesh, R.B. An animal model for studying the pathogenesis of chikungunya virus infection. *Am J Trop Med Hyg.* 2008; 79:133–139.
- 2 Thiberville, S.D.; Moyen, N.; Dupuis-Maguiraga, L.; Nougairede, A.; Gould, E.; Roques, P.; de Lambellerie, X. Chikungunya fever: Epidemiology, clinical syndrome, pathogenesis and therapy. *Antivir Res.* 2013; 99:345-370.
- 3 Powers, A.M. Risks to the Americas associated with the continued expansion of chikungunya virus. *J Gen Virol.* 2015; 96:1-5.

- 4 Weaver, S.C.; Forrester, N.L. Chikungunya: Evolutionary history and recent epidemic spread. *Antivir Res.* 2015; 120:32-39.
- 5 Wahid, B.; Ali, A.; Rafique, S.; Idrees, M. Global expansion of chikungunya virus: mapping the 64-year history. *Int J Infect Dis.* 2017; 58:69-76.
- 6 Abdelnabi, R.; Neyts, J.; Delang, L. Towards antivirals against chikungunya virus. *Antivir Res.* 2015; 121:59-68.
- 7 Abdelnabi, R.; Neyts, J.; Delang, L. Chikungunya virus infections: time to act, time to treat. *Curr Opin Virol.* 2017; 24:25-30.
- 8 Bassetto, M.; De Burghgrave, T.; Delang, L.; Massarotti, A.; Coluccia, A.; Zonta, N.; Gatti, V.; Colombano, G.; Sorba, G.; Silvestri, R.; Tron, G.C.; Neyts, J.; Leyssen, P.; Brancale, A. Computer-aided identification, design and synthesis of a novel series of compounds with selective antiviral activity against chikungunya virus. *Antiviral Res.* 2013; 98:12-18.
- 9 Kale, S.C.; Kale, M.K.; Biyani, K.R. Synthesis of some new benzimidazole acetic acid derivatives and evaluation for their antimicrobial and antitubercular activities. *Tet Letters.* 2013; 54:5370-5373.
- 10 Zhang, L.; Geng, Y.; Jin, Z. Transition-metal-free synthesis of N-aryl hydroxamic acids via insertion of arynes. *J Org Chem.* 2016; 81:3542-3552.
- 11 Narasimhan, B.; Belsare, D.; Pharande, D.; Mourya, V.; Dhake, A. Esters, amides and substituted derivatives of cinnamic acid: synthesis, antimicrobial activity and QSAR investigations. *Eur J Med Chem.* 2004, 39:827-834.
- 12 Kumar, D.; Narang, R.; Judge, V.; Kumar, D.; Narasimhan, B. Antimicrobial evaluation of 4-methylsulfanyl benzylidene/3-hydroxy benzylidene hydrazides and QSAR studies. *Med Chem Res.* 2012, 21: 382-394.
- 13 Wadhvani, P.; Afonin, S.; Ieronimo, M.; Buerck, J.; Ulrich, A.S. Optimised protocol for synthesis of cyclic gramicidin S: starting amine acid is key to high yield. *J Org Chem.* 2006, 71:55-61.
- 14 Pandarus, V.; Gingras, G.; Beland, F.; Ciriminna, R.; Pagliaro, M. Selective hydrogenation of alkenes under ultramild conditions. *Org Process Res Dev.* 2012; 16:1230-1234.
- 15 Carvalho, S.A.; Feitosa, L.O.; Soares, M.; Costa, T.E.M.M.; Henriques, M.G.; Salomao, K.; de Castro, S.L.; Kaiser, M.; Brun, R.; Wardell, J.L.; Wardell, S.M.S.V.; Trossini, G.H.G.; Andricopulo, A.D.; da Silva, E.F.; Fraga, C.A.M. Design and synthesis of new (E)-cinnamic N-acylhydrazones as potent antitrypanosomal agents. *Eur J Med Chem.* 2012; 54:512-521.
- 16 Khan, M.; Santosh, S.R.; Tiwari, M.; Lakshmana Rao, P.V.; Parida, M. Assessment of in vitro prophylactic and therapeutic efficacy of chloroquine against chikungunya virus in vero cells. *J Med Virol.* 2010; 82:817-824.
- 17 Kumar Das, P.; Puusepp, L.; Varghese F.S.; Utt, A.; Ahola, T.; Kananovich, D.G.; Lopp, M.; Merits, A.; Karelson, M. Design and validation of novel chikungunya virus protease inhibitors. *Antimicrob Agents Chemother* 2016; 60:7382-7395.
- 18 Schrödinger Release 2017-1: Glide, Schrödinger, LLC, New York, NY, 2017.
- 19 Halgren, T.A.; Banks, J.L.; Murphy, R.B.; Halgren, T.A.; Klicic, J.J.; Mainz, D.T.; Repasky, M. P.; Knoll, E.H.; Shaw, D.E.; Shelley, M.; Perry, J.K.; Francis, P.; Shenkin, P.S. Glide: A new

approach for rapid, accurate docking and scoring. 1. Method and assessment of docking accuracy. *J Med Chem.* 2004; 47:1739-1749.

Supporting Information

Design, synthesis and evaluation against Chikungunya virus of novel small-molecule antiviral agents

Roberta Tardugno^a, Gilda Giancotti^a, Tine De Burghgraeve^b, Leen Delang^b, Johan Neyts^b, Pieter Leysen^b, Andrea Brancale^a, Marcella Bassetto^{a2}

^aCardiff School of Pharmacy and Pharmaceutical Sciences, Cardiff, King Edward VII Avenue, Cardiff CF103NB, UK

^bRega Institute for Medical Research, University of Leuven, Belgium

Contents

Chemistry materials and methods.

Preparation and characterisation of final products **3, 7-9**.

Molecular modelling methodologies.

Biological assay protocols.

² Corresponding author

E-mail address: bassettom@cardiff.ac.uk (Dr. M. Bassetto)

S.1 Chemistry materials and methods

All solvents used for chromatography were HPLC grade from Fisher Scientific (UK). ^1H and ^{13}C NMR spectra were recorded with a Bruker Avance DPX500 spectrometer operating at 500 and 125 MHz, with Me_4Si as internal standard. Mass spectra were determined with a Bruker microTOF spectrometer using electrospray ionization (ESI source). For mass spectra, solutions were made in HPLC grade methanol. Flash column chromatography was performed with silica gel 60 (230-400mesh) (Merck) and TLC was carried out on precoated silica plates (kiesel gel 60 F₂₅₄, BDH). Compounds were visualised by illumination under UV light (254 nm). Melting points were determined on an electrothermal instrument and are uncorrected. All solvents were dried prior to use and stored over 4 Å molecular sieves, under nitrogen. Purity of prepared compounds was determined by HPLC-UV analysis (Thermo HPLC connected with UV detector). All compounds tested in biological assays were >95% pure. The purity of all final compounds was determined to be >95% by HPLC using the eluents water (eluent A), acetonitrile (eluent B), at the following conditions: Varian Pursuit, 150 mm × 4.6 mm, 5.0 μm, 1.0 mL/min, gradient 30 min 10% → 100% eluent B in eluent A.

Intermediates **4**, **5**, **9a-c**, **10a-c** and **27-28** were prepared according to previously reported procedures.^{S1-S2} Preparation and characterisation of all final products are detailed below. Most hydrazone final products show two sets of signals in NMR experiments.

S.1.1 General method for the preparation of hydrazones **6**, **7**, **11-24**, **29-32**

A mixture of the appropriate hydrazide (1 eq) and the differently substituted benzaldehyde or acetophenone (1.2 eq) in EtOH (8.5 ml · mmol/eq) was refluxed overnight or for 24 hours. The mixture was then cooled to room temperature and the precipitate formed was filtered and washed with cold EtOH and hexane. The solid obtained was purified by crystallization or flash column chromatography.

S.1.1.1 (E)-2-(4-(*tert*-Butyl)phenyl)-*N'*-(4-methoxybenzylidene)cyclopropanecarbohydrazide (**6**)

Purified by flash column chromatography eluting with *n*-hexane-EtOAc 100:0 v/v increasing to *n*-hexane-EtOAc 70:30 v/v. Obtained in 76% yield as a white solid. M.p. 175-179 °C. TLC (8:2 *n*-hexane-EtOAc, Rf: 0.35). Two sets of signals observed in NMR experiments. ^1H -NMR (DMSO- d_6), δ : 1.25 (s, 9H), 1.28 (s, 9H), 1.29-1.39 (m, 2H), 1.45-1.55 (m, 2H), 1.84-1.89 (m, 1H), 2.28-2.31 (m, 1H), 2.37-2.41 (m, 1H), 2.86-2.89 (m, 1H), 3.76 (s, 3H), 3.81 (s, 3H), 6.93 (d, J = 8.4 Hz, 2H), 7.01 (d, J = 8.3 Hz, 2H), 7.10 (d, J = 8.2 Hz, 2H), 7.12 (d, J = 8.3 Hz, 2H), 7.28-7.32 (m, 4H), 7.55 (d, J = 8.0 Hz, 2H), 7.63 (d, J = 8.0 Hz, 2H), 7.95 (s, 1H), 8.07 (s, 1H), 11.30 (bs, 1H), 11.49 (bs, 1H). ^{13}C -NMR (DMSO- d_6), δ : 14.8, 16.4, 21.5, 24.2, 24.8, 24.9, 31.1, 34.0, 55.2, 55.3, 114.2, 114.3, 125.0, 125.1, 125.5, 125.7, 126.7, 126.8, 128.1, 128.5, 137.6, 137.7, 143.0, 145.5, 148.5, 160.4, 160.6, 167.4, 172.6. Anal. Calcd for C₂₂H₂₆N₂O₂: C, 75.40; H, 7.48; N, 7.99. Found: C, 75.47; H, 7.26; N, 7.84. MS [ESI, m/z]: 351.2 [M+H].

S.1.1.2 (E)-2-(4-(*tert*-Butyl)phenyl)-*N'*-(4-hydroxybenzylidene)cyclopropanecarbohydrazide (**7**)

Purified by flash column chromatography eluting with *n*-hexane-EtOAc 100:0 v/v increasing to *n*-hexane-EtOAc 90:10 v/v. Obtained in 54% yield as a pale yellow. M.p. 198-200 °C. TLC (5:5 *n*-hexane-EtOAc, Rf: 0.41). Two sets of signals observed in NMR experiments. ^1H -NMR (DMSO- d_6), δ : 1.24 (s,

9 H), 1.27 (s, 9H), 1.30-1.44 (m, 2H), 1.46-1.50 (m, 2H), 1.80-1.85 (m, 1H), 2.23-2.28 (m, 1H), 2.36-2.41 (m, 1H), 2.83-2.89 (m, 1H), 6.73-6.82 (m, 4H), 7.08 (d, J= 8.3 Hz, 2H), 7.11 (d, J= 8.2 Hz, 2H), 7.27-7.31 (m, 4H), 7.46 (d, J= 8.1 Hz, 2H), 7.52 (d, J= 8.1 Hz, 2H), 7.92 (s, 1H), 8.04 (s, 1H), 9.85 (bs, 2H), 11.22 (bs, 1H), 11.41 (bs, 1H). ¹³C-NMR (DMSO-d₆), δ: 14.0, 16.3, 21.5, 24.1, 24.8, 24.9, 31.1, 34.0, 115.6, 115.6, 125.0, 125.1, 125.2, 125.3, 125.5, 125.7, 128.3, 128.6, 137.6, 137.7, 143.4, 145.9, 148.4, 159.0, 159.2, 167.2, 172.5. Anal. Calcd for C₂₁H₂₄N₂O₂: C, 74.97; H, 7.19; N, 8.33. Found: C, 75.13; H, 7.31; N, 8.11. MS [ESI, m/z]: 337.2 [M+H].

S.1.1.3 (2-E)-3-(4-(*tert*-Butyl)phenyl)-*N'*-(4-methoxybenzylidene)acrylohydrazide (**11a**)

Purified by flash column chromatography eluting with *n*-hexane-EtOAc 100:0 v/v increasing to *n*-hexane-EtOAc 50:50 v/v. Obtained in 71% yield as an off-white solid. M.p. 186-188 °C. TLC (5:5 *n*-hexane-EtOAc, Rf: 0.40). Two sets of signals observed in NMR experiments. ¹H-NMR (DMSO-d₆), δ: 1.29 (s, 9H), 1.30 (s, 9H), 3.81 (s, 6H), 6.67 (d, J= 15.7 Hz, 1H), 7.01 (d, J= 8.1 Hz, 4H), 7.44-7.48 (m, 4H), 7.54-7.58 (m, 4H), 7.60-7.66 (m, 2H), 7.67-7.72 (m, 5H), 8.02 (s, 1H), 8.20 (s, 1H), 11.36 (bs, 1H), 11.52 (bs, 1H). ¹³C-NMR (DMSO-d₆), δ: 30.9, 34.5, 55.2, 55.3, 114.2, 116.5, 119.4, 125.7, 125.8, 126.8, 126.9, 127.5, 127.9, 128.4, 128.6, 131.9, 132.2, 140.1, 141.6, 142.8, 146.4, 152.6, 152.7, 160.6, 160.8, 161.4, 165.9. Anal. Calcd for C₂₁H₂₄N₂O₂: C, 74.97; H, 7.19; N, 8.33. Found: C, 74.81; H, 7.40; N, 8.42. MS [ESI, m/z]: 359.1 [M+Na].

S.1.1.4 (2-E)-3-(4-(*tert*-Butyl)phenyl)-*N'*-(4-methylbenzylidene)acrylohydrazide (**12a**)

Purified by flash column chromatography eluting with *n*-hexane-EtOAc 100:0 v/v increasing to *n*-hexane-EtOAc 50:50 v/v. Obtained in 77% yield as an off-white solid. M.p. 200-202 °C. TLC (6:4 *n*-hexane-EtOAc, Rf: 0.44). Two sets of signals observed in NMR experiments. ¹H-NMR (DMSO-d₆), δ: 1.29 (s, 9H), 1.30 (s, 9H), 2.34 (s, 6H), 6.68 (d, J= 15.8 Hz, 1H), 7.26 (d, J= 7.9 Hz, 4H), 7.43-7.49 (m, 3H), 7.51-7.58 (m, 4H), 7.61-7.70 (m, 8H), 8.04 (s, 1H), 8.23 (s, 1H), 11.42 (bs, 1H), 11.59 (bs, 1H). ¹³C-NMR (DMSO-d₆), δ: 21.0, 30.9, 34.5, 116.4, 119.4, 125.7, 125.8, 126.8, 127.1, 127.5, 127.9, 129.4, 131.5, 131.6, 131.9, 132.1, 139.5, 139.8, 140.2, 141.8, 143.1, 146.6, 152.6. Anal. Calcd for C₂₁H₂₄N₂O₂: C, 74.97; H, 7.19; N, 8.33. Found: C, 74.81; H, 7.40; N, 8.42. MS [ESI, m/z]: 359.1 [M+Na].

S.1.1.5 (2E)-*N'*-(4-Methylbenzylidene)-3-(*p*-tolyl)acrylohydrazide (**12b**)

Purified by flash column chromatography eluting with *n*-hexane-EtOAc 100:0 v/v increasing to *n*-hexane-EtOAc 50:50 v/v. Obtained in 67% yield as an off-white solid. M.p. 232-234 °C. TLC (5:5 *n*-hexane-EtOAc, Rf: 0.32). Two sets of signals observed in NMR experiments. ¹H-NMR (DMSO-d₆), δ: 2.32 (s, 6H), 2.37 (s, 6H), 6.65 (d, J= 15.7 Hz, 1H), 7.24-7.31 (m, 8H), 7.50-7.54 (m, 3H), 7.57 (d, J= 15.7 Hz, 1H), 7.60-7.68 (m, 7H), 8.03 (s, 1H), 8.22 (s, 1H), 11.40 (bs, 1H), 11.56 (bs, 1H). ¹³C-NMR (DMSO-d₆), δ: 20.9, 21.0, 116.1, 118.3, 119.2, 126.8, 127.0, 127.6, 127.7, 128.1, 129.3, 129.5, 131.4, 131.6, 131.9, 132.1, 139.5, 139.6, 139.8, 139.9, 140.4, 141.9, 143.1, 146.6, 161.4, 166.0. Anal. Calcd for C₁₈H₁₈N₂O: C, 77.67; H, 6.52; N, 10.06. Found: C, 77.51; H, 6.27; N, 10.24. MS [ESI, m/z]: 279.1 [M+H].

S.1.1.6 *N'*-(4-Methylbenzylidene)cinnamohydrazide (**12c**)

Purified by flash column chromatography eluting with *n*-hexane-EtOAc 100:0 v/v increasing to *n*-hexane-EtOAc 50:50 v/v. Obtained in 71% yield as an off-white solid. M.p. 204-206 °C. TLC (5:5 *n*-hexane-EtOAc, Rf: 0.34). One set of signals observed in NMR experiments. ¹H-NMR (CDCl₃), δ: 2.43 (s, 3H), 7.34-7.19 (m, 2H), 7.48-7.37 (m, 3H), 7.73-7.54 (m, 5H), 7.86 (s, 1H), 7.90 (d, J= 16.0 Hz, 1H); 9.47 (bs, 1H). ¹³C-NMR (CDCl₃), δ: 21.5, 116.5, 127.2, 128.3, 128.8, 128.9, 129.5, 130.0, 131.0, 135.1, 140.5, 143.7, 167.3. Anal. Calcd for C₁₇H₁₆N₂O: C, 77.25; H, 6.10; N, 10.60. Found: C, 77.12; H, 6.39; N, 10.37. MS [ESI, m/z]: 265.1 [M+H].

S.1.1.7 (2E)-3-(4-(*tert*-Butyl)phenyl)-*N'*-(4-isopropylbenzylidene)acrylohydrazide (**13a**)

Purified by flash column chromatography eluting with *n*-hexane-EtOAc 100:0 v/v increasing to *n*-hexane-EtOAc 50:50 v/v. Obtained in 77% yield as an off-white solid. M.p. 223-225 °C. TLC (5:5 *n*-hexane-EtOAc, Rf: 0.55). Two sets of signals observed in NMR experiments. ¹H-NMR (DMSO-d₆), δ: 1.22 (d, J= 6.8 Hz, 12H), 1.29 (s, 9H), 1.30 (s, 9H), 3.01-2.85 (m, 2H), 6.68 (d, J= 15.8 Hz, 1H), 7.29-7.35 (m, 4H), 7.43-7.50 (m, 4H), 7.52-7.64 (m, 5H), 7.65-7.72 (m, 6H), 8.05 (s, 1H), 8.24 (s, 1H), 11.43 (s, 1H), 11.59 (s, 1H). ¹³C-NMR (DMSO-d₆), δ: 23.6, 30.9, 33.3, 33.4, 34.5, 116.4, 119.3, 125.7, 125.7, 126.7, 126.9, 127.1, 127.5, 127.9, 131.9, 132.0, 132.1, 140.2, 141.7, 143.0, 146.5, 150.2, 150.6, 152.6, 152.7, 161.4, 166.0. Anal. Calcd for C₂₃H₂₂N₂O: C, 77.27; H, 8.10; N, 8.04. Found: C, 77.49; H, 8.25; N, 7.87. MS [ESI, m/z]: 349.2 [M+H].

S.1.1.8 (2E)-*N'*-(4-(*tert*-Butyl)benzylidene)-3-(4-(*tert*-butyl)phenyl)acrylohydrazide (**14a**)

Purified by flash column chromatography eluting with *n*-hexane-EtOAc 100:0 v/v increasing to *n*-hexane-EtOAc 50:50 v/v. Obtained in 68% yield as an off-white solid. M.p. 223-225 °C. TLC (6:4 *n*-hexane-EtOAc, Rf: 0.52). Two sets of signals observed in NMR experiments. ¹H-NMR (DMSO-d₆), δ: 1.29 (s, 18H), 1.31 (s, 18H), 6.69 (d, J= 15.7 Hz, 1H), 7.39-7.50 (m, 7H), 7.52-7.58 (m, 3H), 7.58-7.62 (m, 2H), 7.62-7.71 (m, 7H), 8.05 (s, 1H), 8.25 (s, 1H), 11.46 (bs, 1H), 11.60 (bs, 1H). ¹³C-NMR (DMSO-d₆), δ: 30.8, 30.9, 31.0, 31.2, 34.5, 116.4, 119.3, 125.5, 125.6, 125.7, 126.6, 126.9, 127.5, 127.9, 131.5, 131.9, 132.1, 140.3, 141.7, 142.8, 146.5, 152.4, 152.6, 152.7, 161.5, 166.0. Anal. Calcd for C₂₄H₃₀N₂O: C, 79.52; H, 8.34; N, 7.73. Found: C, 79.45; H, 8.51; N, 7.87. MS [ESI, m/z]: 363.2 [M+H].

S.1.1.9 (2E)-3-(4-(*tert*-Butyl)phenyl)-*N'*-(1-(4-cyclohexylphenyl)ethylidene)acrylohydrazide (**15a**)

Purified by flash column chromatography eluting with *n*-hexane-EtOAc 100:0 v/v increasing to *n*-hexane-EtOAc 50:50 v/v. Obtained in 65% yield as a pale yellow solid. M.p. 258-260 °C. TLC (6:4 *n*-hexane-EtOAc, Rf: 0.45). One set of signals observed in NMR experiments. ¹H-NMR (CDCl₃), δ: 1.35-1.30 (m, 2H), 1.38 (s, 9H), 1.47-1.45 (m, 4H), 2.32 (s, 3H), 2.66-2.51 (m, 1H), 7.31 (d, J= 8.3 Hz, 2H), 7.46 (d, J= 8.5 Hz, 2H), 7.60-7.65 (m, 3H), 7.76 (d, J= 8.3, 2H), 7.89 (d, J= 15.9 Hz, 1H), 9.10 (bs, 1H, NH). ¹³C-NMR (CDCl₃), δ: 12.8, 26.1, 26.8, 31.1, 34.3, 34.9, 44.4, 116.0, 125.8, 126.2, 126.6, 127.0, 128.2, 132.6, 135.8, 147.3, 149.6, 153.5, 167.9. Anal. Calcd for C₂₇H₃₄N₂O: C, 80.55; H, 8.51; N, 6.96. Found: C, 80.66; H, 8.37; N, 7.13. MS [ESI, m/z]: 403.3 [M+H].

S.1.1.10 (1-(4-Cyclohexylphenyl)ethylidene)cinnamohydrazide (**15c**)

Purified by flash column chromatography eluting with *n*-hexane-EtOAc 100:0 v/v increasing to *n*-hexane-EtOAc 50:50 v/v. Obtained in 69% yield as a pale yellow solid. M.p. 240-242 °C. TLC (5:5 *n*-hexane-EtOAc, Rf: 0.40). One set of signals observed in NMR experiments. ¹H-NMR (CDCl₃), δ: 1.36-1.26 (m, 1H), 1.54-1.38 (m, 4H), 1.80 (m, 1H), 1.99-1.84 (m, 4H), 2.31 (s, 3H), 2.64-2.53 (m, 1H), 7.31 (d, J= 8.1 Hz, 2H), 7.47-7.40 (m, 3H), 7.70-7.63 (m, 3H), 7.75 (d, J= 8.1, 2H), 7.89 (d, J= 15.8 Hz, 1H), 8.91 (s, 1H, NH). ¹³C-NMR (CDCl₃), δ: 26.1, 26.8, 34.3, 44.4, 116.8, 126.2, 127.0, 128.3, 128.8, 130.0, 132.2, 135.6, 143.7, 149.4, 149.7, 167.5. Anal. Calcd for C₂₃H₂₆N₂O: C, 79.73; H, 7.56; N, 8.09. Found: C, 79.49; H, 7.41; N, 8.30. MS [ESI, m/z]: 347.2 [M+H].

S.1.1.11 (2E)-*N'*-Benzylidene-3-(4-(*tert*-butyl)phenyl)acrylohydrazide (**16a**)

Purified by flash column chromatography eluting with *n*-hexane-EtOAc 100:0 v/v increasing to *n*-hexane-EtOAc 50:50 v/v. Obtained in 73% yield as an off-white solid. M.p. 227-229 °C. TLC (5:5 *n*-hexane-EtOAc, Rf: 0.45). Two sets of signals observed in NMR experiments. ¹H-NMR (DMSO-*d*₆), δ: 1.29 (s, 9H), 1.30 (s, 9H), 6.68 (d, J= 15.7 Hz, 1H), 7.41-7.48 (m, 10H), 7.54-7.59 (m, 3H), 7.62 (d, J= 15.7, 1H), 7.65-7.70 (m, 3H), 7.72-7.78 (m, 4H), 8.08 (s, 1H), 8.27 (s, 1H), 11.49 (bs, 1H), 11.66 (bs, 1H). ¹³C-NMR (DMSO-*d*₆), δ: 30.9, 34.53, 116.3, 119.2, 125.7, 125.8, 126.8, 127.0, 127.5, 127.9, 128.7, 129.7, 129.9, 131.9, 132.1, 134.2, 134.3, 140.4, 141.9, 143.0, 146.6, 152.7, 152.8, 161.6, 166.1. Anal. Calcd for C₂₀H₂₂N₂O: C, 78.40; H, 7.24; N, 9.14. Found: C, 78.67; H, 6.99; N, 8.88. MS [ESI, m/z]: 307.2 [M+H].

S.1.1.12 (2E)-3-(4-(*tert*-Butyl)phenyl)-*N'*-(4-nitrobenzylidene)acrylohydrazide (**17a**)

Purified by flash column chromatography eluting with *n*-hexane-EtOAc 100:0 v/v increasing to *n*-hexane-EtOAc 50:50 v/v. Obtained in 70% yield as a pale yellow solid. M.p. 230-232 °C. TLC (5:5 *n*-hexane-EtOAc, Rf: 0.35). Two sets of signals observed in NMR experiments. ¹H-NMR (DMSO-*d*₆), δ: 1.30 (s, 18H), 6.68 (d, J= 15.7 Hz, 1H), 7.41-7.48 (m, 4H), 7.53-7.60 (m, 3H), 7.73-7.81 (m, 4H), 7.88-8.07 (m, 4H), 8.16 (s, 1H), 8.24-8.31 (m, 4H), 8.36 (s, 1H), 11.79 (bs, 1H), 11.94 (bs, 1H). ¹³C-NMR (DMSO-*d*₆), δ: 30.9, 34.5, 115.9, 118.91, 123.9, 125.6, 125.7, 125.8, 127.7, 127.8, 127.9, 128.1, 131.8, 132.0, 140.5, 140.6, 140.7, 141.1, 142.6, 144.0, 147.6, 147.7, 152.9, 153.0, 161.9, 166.5. Anal. Calcd for C₂₀H₂₁N₃O₃: C, 68.36; H, 6.02; N, 11.96. Found: C, 68.12; H, 5.89; N, 12.21. MS [ESI, m/z]: 352.2 [M+H].

S.1.1.13 (2E)-3-(4-(*tert*-Butyl)phenyl)-*N'*-(1-(4-chlorophenyl)ethylidene)acrylohydrazide (**18a**)

Purified by flash column chromatography eluting with *n*-hexane-EtOAc 100:0 v/v increasing to *n*-hexane-EtOAc 50:50 v/v. Obtained in 72% yield as an off-white solid. M.p. 244-246 °C. TLC (5:5 *n*-hexane-EtOAc, Rf: 0.41). Two sets of signals observed in NMR experiments. ¹H-NMR (DMSO-*d*₆), δ: 1.30 (s, 18H), 2.30 (s, 3H), 2.33 (s, 3H), 7.02 (d, J= 15.6 Hz, 1H), 7.45-7.51 (m, 8H), 7.53-7.60 (m, 4H), 7.63-7.71 (m, 3H), 7.80-7.95 (m, 4H), 10.62 (bs, 1H), 10.67 (bs, 1H). ¹³C-NMR (DMSO-*d*₆), δ: 13.5, 13.9, 30.9, 34.5, 116.6, 119.7, 125.7, 127.4, 127.5, 127.8, 127.9, 128.1, 128.3, 132.1, 133.8, 137.0, 140.3, 142.0, 152.6. Anal. Calcd for C₂₁H₂₃ClN₂O: C, 71.07; H, 6.53; N, 7.89. Found: C, 71.15; H, 6.50; N,

8.02. MS [ESI, m/z]: 355.2, 357.2 [M+H].

S.1.1.14 (2E)-3-(4-(*tert*-Butyl)phenyl)-*N'*-(4-hydroxybenzylidene)acrylohydrazide (**19a**)

Purified by flash column chromatography eluting with *n*-hexane-EtOAc 100:0 v/v increasing to *n*-hexane-EtOAc 0:100 v/v. Obtained in 69% yield as a pale yellow solid. M.p. 268-270 °C. TLC (3:7 *n*-hexane-EtOAc, Rf: 0.30). Two sets of signals observed in NMR experiments. ¹H-NMR (DMSO-*d*₆), δ: 1.29 (s, 9H), 1.30 (s, 9H), 6.66 (d, J= 16.0 Hz, 1H), 6.82-6.86 (m, 4H), 7.43-7.48 (m, 5H), 7.53-7.60 (m, 7H), 7.62-7.69 (m, 3H), 7.97 (s, 1H), 8.15 (s, 1H), 9.87 (bs, 1H), 9.91 (bs, 1H), 11.28 (bs, 1H), 11.45 (bs, 1H). ¹³C-NMR (DMSO-*d*₆), δ: 30.9, 34.5, 115.6, 116.6, 118.5, 119.5, 125.2, 125.3, 125.7, 125.8, 127.4, 127.9, 128.5, 128.8, 131.9, 132.2, 139.9, 141.4, 143.2, 146.8, 152.5, 152.7, 159.1, 159.3, 161.2, 165.8. Anal. Calcd for C₂₀H₂₂N₂O₂: C, 74.51; H, 6.88; N, 8.69. Found: C, 74.62; H, 6.59; N, 8.54. MS [ESI, m/z]: 323.2 [M+H].

S.1.1.15 (2E)-3-(4-(*tert*-Butyl)phenyl)-*N'*-(1-(pyrazin-2-yl)ethylidene)acrylohydrazide (**20a**)

Purified by flash column chromatography eluting with *n*-hexane-EtOAc 100:0 v/v increasing to *n*-hexane-EtOAc 0:100 v/v. Obtained in 74% yield as an off-white solid. M.p. 230-232 °C. TLC (4:6 *n*-hexane-EtOAc, Rf: 0.28). Two sets of signals observed in NMR experiments. ¹H-NMR (CDCl₃), δ: 1.31 (s, 9H), 1.37 (s, 9H), 2.46 (s, 6H), 6.94 (d, J= 15.7 Hz, 1H), 7.33 (d, J= 8.4 Hz, 2H), 7.41-7.49 (m, 3H), 7.52 (d, J= 8.4, 2H), 7.57-7.69 (m, 4H), 7.76 (d, J= 15.7, 1H), 7.93 (d, J= 15.7, 1H), 8.56 (apparent s, 3H), 9.29 (s, 1H), 9.45 (bs, 1H), 10.98 (bs, 1H). ¹³C-NMR (CDCl₃), δ: 10.4, 31.1, 34.8, 115.0, 117.2, 125.8, 127.8, 128.2, 132.0, 132.2, 141.6, 142.8, 143.0, 143.7, 144.7, 146.3, 150.6, 153.9, 161.1, 167.8. Anal. Calcd for C₁₉H₂₂N₄O: C, 70.78; H, 6.88; N, 17.38. Found: C, 70.94; H, 6.61; N, 17.42. MS [ESI, m/z]: 323.2 [M+H].

S.1.1.16 (2E)-3-(4-(*tert*-butyl)phenyl)-*N'*-(1-(3,4-dimethoxyphenyl)ethylidene)acrylohydrazide (**21a**)

Purified by flash column chromatography eluting with *n*-hexane-EtOAc 100:0 v/v increasing to *n*-hexane-EtOAc 40:60 v/v. Obtained in 75% yield as a pale yellow solid. M.p. 200-202 °C. TLC (5:5 *n*-hexane-EtOAc, Rf: 0.23). Two sets of signals observed in NMR experiments. ¹H-NMR (DMSO-*d*₆), δ: 1.30 (s, 18H), 2.28 (s, 3H), 2.32 (s, 3H), 3.80 (s, 6H), 3.81 (s, 3H), 3.87 (s, 3H), 6.97-7.04 (m, 3H), 7.32-7.38 (m, 2H), 7.41-7.50 (m, 6H), 7.52-7.61 (m, 4H), 7.62-7.68 (m, 3H), 10.50 (bs, 1H), 10.58 (bs, 1H). ¹³C-NMR (DMSO-*d*₆), δ: 13.3, 14.1, 30.9, 34.5, 55.3, 55.5, 108.9, 109.4, 111.1, 111.2, 117.0, 118.5, 119.1, 119.7, 120.0, 125.7, 127.4, 127.7, 130.8, 132.2, 139.8, 141.4, 147.2, 148.4, 149.9, 150.1, 151.7, 152.5, 152.5, 161.8, 163.2. Anal. Calcd for C₂₀H₂₂N₂O₂: C, 74.51; H, 6.88; N, 8.69. Found: C, 74.62; H, 6.59; N, 8.54. MS [ESI, m/z]: 323.2 [M+H].

S.1.1.17 (2E)-*N'*-([1,1'-Biphenyl]-4-ylmethylene)-3-(4-(*tert*-butyl)phenyl)acrylohydrazide (**22a**)

Purified by flash column chromatography eluting with *n*-hexane-EtOAc 100:0 v/v increasing to *n*-hexane-EtOAc 50:50 v/v. Obtained in 65% yield as a pale yellow solid. M.p. 218-220 °C. TLC (5:5 *n*-hexane-EtOAc, Rf: 0.30). Two sets of signals observed in NMR experiments. ¹H-NMR (DMSO-*d*₆), δ: 1.30 (s, 9H), 1.31 (s, 9H), 6.69 (d, J= 15.7 Hz, 1H), 7.38-7.43 (m, 2H), 7.46-7.52 (m, 8H), 7.56-7.61 (m,

4H), 7.63-7.71 (m, 3H), 7.72-7.75 (m, 4H), 7.76-7.80 (m, 4H), 7.82-7.87 (m, 4H), 8.11 (s, 1H), 8.30 (s, 1H), 11.52 (bs, 1H), 11.68 (bs, 1H). ¹³C-NMR (DMSO-d₆), δ: 30.9, 34.5, 116.4, 119.3, 125.7, 125.8, 126.6, 126.9, 127.4, 127.5, 127.6, 127.8, 128.0, 129.0, 139.3, 140.4, 141.3, 141.5, 141.9, 142.6, 146.1, 152.7, 152.8, 160.3, 161.5, 166.2. Anal. Calcd for C₂₆H₂₆N₂O: C, 81.64; H, 6.85; N, 7.32. Found: C, 81.51; H, 6.99; N, 7.14. MS [ESI, m/z]: 383.2 [M+H].

S.1.1.18 (2E)-*N'*-(1-([1,1'-Biphenyl]-4-yl)ethylidene)-3-(4-(*tert*-butyl)phenyl)acrylohydrazide (**23a**)

Purified by flash column chromatography eluting with *n*-hexane-EtOAc 100:0 v/v increasing to *n*-hexane-EtOAc 50:50 v/v. Obtained in 68% yield as an off-white solid. M.p. 254-256 °C. TLC (6:4 *n*-hexane-EtOAc, Rf: 0.30). Two sets of signals observed in NMR experiments. ¹H-NMR (DMSO-d₆), δ: 1.31 (s, 18H), 2.34 (s, 3H), 2.37 (s, 3H), 7.04 (d, J = 15.7 Hz, 1H), 7.39-7.44 (m, 2H), 7.47-7.52 (m, 8H), 7.57-7.60 (m, 3H), 7.62-7.69 (m, 4H), 7.72-7.78 (m, 8H), 7.92-7.96 (m, 4H), 10.60 (bs, 1H), 10.68 (bs, 1H). ¹³C-NMR (DMSO-d₆), δ: 14.6, 30.9, 34.5, 117.6, 119.8, 125.8, 126.4, 126.5, 126.9, 127.5, 127.7, 127.9, 128.9, 137.2, 139.2, 140.1, 140.5, 141.3, 142.5, 144.9, 145.7, 146.5, 147.6, 161.4, 164.9, 166.2. Anal. Calcd for C₂₇H₂₈N₂O: C, 81.78; H, 7.12; N, 7.06. Found: C, 81.99; H, 7.35; N, 6.84. MS [ESI, m/z]: 397.2 [M+H].

S.1.1.19 (2E)-*N'*-(3,4-Diethoxybenzylidene)-3-(*p*-tolyl)acrylohydrazide (**24c**)

Purified by flash column chromatography eluting with *n*-hexane-EtOAc 100:0 v/v increasing to *n*-hexane-EtOAc 50:50 v/v. Obtained in 66% yield as a pale yellow solid. M.p. 170-172 °C. TLC (5:5 *n*-hexane-EtOAc, Rf: 0.30). Two sets of signals observed in NMR experiments. ¹H-NMR (CDCl₃), δ: 1.33-1.48 (m, 6H), 1.48-1.59 (m, 6H), 2.37 (s, 3H), 2.42 (s, 3H), 4.06-4.13 (m, 4H), 4.17 (q, J = 6.9 Hz, 2H), 4.22 (q, J = 6.9 Hz, 2H), 6.48 (d, J = 15.5 Hz, 1H), 6.80 (d, J = 6.9 Hz, 1H), 6.93 (d, J = 8.0 Hz, 1H), 7.01-7.11 (m, 3H), 7.34-7.42 (m, 3H), 7.55-7.64 (m, 3H), 7.87 (s, 1H), 7.89 (s, 2H), 8.15 (s, 1H), 9.34 (bs, 1H), 9.99 (bs, 1H). ¹³C-NMR (CDCl₃), δ: 14.7, 14.8, 21.5, 64.5, 64.7, 111.1, 112.7, 115.7, 121.6, 126.7, 128.3, 129.6, 132.5, 140.4, 143.5, 143.9, 148.9, 150.8, 167.7. Anal. Calcd for C₂₁H₂₄N₂O₃: C, 71.57; H, 6.86; N, 7.95. Found: C, 71.33; H, 6.99; N, 8.04. MS [ESI, m/z]: 353.2 [M+H].

S.1.1.20 3-(4-(*tert*-Butyl)phenyl)-*N'*-(3,4-diethoxybenzylidene)propanehydrazide (**29a**)

Purified by crystallization from EtOH. Obtained in 79% yield as a white solid. M.p. 108-112 °C. TLC (5:5 *n*-hexane-EtOAc, Rf: 0.61). Two sets of signals observed in NMR experiments. ¹H-NMR (DMSO-d₆), δ: 1.25 (s, 9H), 1.26 (s, 9H), 1.31-1.37 (m, 12H), 2.46-2.49 (m, 2H), 2.83-2.89 (m, 6H), 4.02-4.08 (m, 8H), 6.96-7.00 (m, 2H), 7.10-7.14 (m, 2H), 7.15 (d, J = 8.2 Hz, 2H), 7.19 (d, J = 8.2 Hz, 2H), 7.24 (d, J = 1.8 Hz, 1H), 7.26 (d, J = 1.8 Hz, 1H), 7.27-7.31 (m, 4H), 7.87 (s, 1H), 8.04 (s, 1H), 11.16 (bs, 1H), 11.23 (bs, 1H). ¹³C-NMR (DMSO-d₆), δ: 14.6, 14.7, 31.2, 29.7, 33.9, 63.6, 63.7, 109.6, 112.5, 120.7, 121.5, 124.9, 127.8, 142.6, 146.0, 126.9, 137.9, 148.1, 149.7, 167.5, 173.3. Anal. Calcd for C₂₄H₃₂N₂O₃: C, 72.70; H, 8.13; N, 7.06. Found: C, 72.95; H, 8.17; N, 6.88. MS [ESI, m/z]: 397.1 [M+H].

S.1.1.21 *N'*-(3,4-Diethoxybenzylidene)-3-phenylpropanehydrazide (**29c**)

Purified by crystallization from EtOH. Obtained in 77% yield as a white solid. M.p. 94-98 °C. TLC (3:7

n-hexane-EtOAc, Rf: 0.72). Two sets of signals observed in NMR experiments. ¹H-NMR (DMSO-d₆), δ: 1.31-1.36 (m, 12H), 2.52-2.55 (m, 2H), 2.87-2.92 (m, 6H), 4.01-4.08 (m, 8H), 6.96-7.00 (m, 2H), 7.10-7.14 (m, 2H), 7.16-7.21 (m, 2H), 7.23-7.25 (m, 3H), 7.26-7.31 (m, 7H), 7.88 (s, 1H), 8.04 (s, 1H), 11.17 (bs, 1H), 11.24 (bs, 1H). ¹³C-NMR (DMSO-d₆), δ: 14.6, 14.7, 30.1, 30.7, 33.8, 35.7, 109.7, 112.6, 120.7, 121.5, 125.8, 125.9, 126.8, 142.7, 146.1, 126.9, 141.0, 148.2, 149.9, 173.2. Anal. Calcd for C₂₀H₂₄N₂O₃: C, 70.56; H, 7.11; N, 8.23. Found: C, 70.69; H, 7.33; N, 8.05. MS [ESI, m/z]: 341.0 [M+H].

S.1.1.22 3-(4-(*tert*-Butyl)phenyl)-*N'*-(4-methylbenzylidene)propanehydrazide (**30a**)

Purified by crystallization from EtOH. Obtained in 81% yield as a white solid. M.p. 113-115 °C. TLC (5:5 *n*-hexane-EtOAc, Rf: 0.66). Two sets of signals observed in NMR experiments. ¹H-NMR (DMSO-d₆), δ: 1.33 (s, 18H), 2.39 (s, 3H), 2.41 (s, 3H), 2.60-2.64 (m, 2H), 3.04-3.08 (m, 4H), 3.10-3.14 (m, 2H), 7.19-7.20 (m, 2H), 7.23 (d, J = 8.1 Hz, 4H), 7.26 (d, J = 8.3 Hz, 2H), 7.36 (d, J = 8.3 Hz, 4H), 7.57 (d, J = 8.1 Hz, 4H), 7.62 (d, J = 8.1 Hz, 2H), 7.79 (s, 1H), 7.96 (s, 1H), 8.48 (bs, 1H), 9.73 (bs, 1H). ¹³C-NMR (DMSO-d₆), δ: 21.5, 31.0, 30.2, 34.6, 34.4, 125.3, 125.5, 127.1, 127.6, 143.7, 128.1, 138.1, 140.4, 148.9, 175.4. Anal. Calcd for C₂₁H₂₆N₂O: C, 78.22; H, 8.13; N, 8.69. Found: C, 77.97; H, 8.26; N, 8.88. MS [ESI, m/z]: 323.1 [M+H].

S.1.1.23 *N'*-(4-Methylbenzylidene)-3-phenylpropanehydrazide (**30c**)

Purified by crystallization from EtOH. Obtained in 92% yield as a white solid. M.p. 91-95 °C. TLC (3:7 *n*-hexane-EtOAc, Rf: 0.65). Two sets of signals observed in NMR experiments. ¹H-NMR (DMSO-d₆), δ: 2.32 (s, 3H), 2.33 (s, 3H), 2.52-2.53 (m, 2H), 2.88-2.95 (m, 6H), 7.16-7.20 (m, 2H), 7.21-7.26 (m, 6H), 7.27-7.31 (m, 6H), 7.52 (d, J = 7.9 Hz, 2H), 7.56 (d, J = 7.8 Hz, 2H), 7.95 (s, 1H), 8.10 (s, 1H), 11.22 (bs, 1H), 11.31 (bs, 1H). ¹³C-NMR (DMSO-d₆), δ: 20.9, 29.9, 33.7, 125.8, 126.5, 126.9, 128.2, 128.3, 129.3, 129.4, 145.8, 131.5, 139.3, 141.0, 173.3. Anal. Calcd for C₁₇H₁₈N₂O: C, 76.66; H, 6.81; N, 10.52. Found: C, 76.43; H, 6.59; N, 10.74. MS [ESI, m/z]: 267.0 [M+H].

S.1.1.24 3-(4-(*tert*-butyl)phenyl)-*N'*-(4-hydroxybenzylidene)propanehydrazide (**31a**)

Purified by crystallization from EtOH. Obtained in 95% yield as a white solid. M.p. 165-169 °C. TLC (5:5 *n*-hexane-EtOAc, Rf: 0.51). Two sets of signals observed in NMR experiments. ¹H-NMR (DMSO-d₆), δ: 1.25 (s, 18H), 2.47 (t, J = 7.6 Hz, 2H), 2.83-2.91 (m, 6H), 6.78-6.82 (m, 4H), 7.15 (d, J = 8.1 Hz, 2H), 7.18 (d, J = 8.1 Hz, 2H), 7.28-7.31 (m, 4H), 7.46 (d, J = 8.5 Hz, 2H), 7.50 (d, J = 8.5 Hz, 2H), 7.86 (s, 1H), 8.03 (s, 1H), 9.88 (bs, 2H), 11.06 (bs, 1H), 11.16 (bs, 1H). ¹³C-NMR (DMSO-d₆), δ: 29.5, 33.7, 31.2, 35.7, 115.7, 127.9, 128.2, 128.6, 146.1, 124.9, 137.9, 148.1, 159.2, 173.1. Anal. Calcd for C₂₀H₂₄N₂O₂: C, 74.04; H, 7.46; N, 8.64. Found: C, 73.85; H, 7.71; N, 8.47. MS [ESI, m/z]: 325.0 [M+H].

S.1.1.25 *N'*-(4-hydroxybenzylidene)-3-phenylpropanehydrazide (**31c**)

Purified by crystallization from EtOH. Obtained in 88% yield as a white solid. M.p. 135-139 °C. TLC (3:7 *n*-hexane-EtOAc, Rf: 0.60). Two sets of signals observed in NMR experiments. ¹H-NMR (DMSO-d₆), δ: 2.53-2.62 (m, 2H), 2.86-2.95 (m, 6H), 6.78-6.83 (m, 4H), 7.16-7.21 (m, 2H), 7.22-7.31 (m, 8H), 7.46 (d, J = 8.1 Hz, 2H), 7.50 (d, J = 8.1 Hz, 2H), 7.87 (s, 1H), 8.02 (s, 1H), 9.88 (bs, 2H), 11.08 (bs,

1H), 11.16 (bs, 1H). ¹³C-NMR (DMSO-d₆), δ: 30.0, 33.7, 115.5, 115.6, 125.8, 125.9, 128.2, 128.3, 128.4, 128.7, 142.8, 146.1, 125.2, 141.4, 159.2, 173.1. Anal. Calcd for C₁₆H₁₆N₂O₂: C, 71.62; H, 6.01; N, 10.44. Found: C, 71.90; H, 5.98; N, 10.35. MS [ESI, m/z]: 269.0 [M+H].

S.1.1.26 3-(4-(*tert*-Butyl)phenyl)-*N'*-(1-(4-cyclohexylphenyl)ethylidene)propanehydrazide (**32a**)

Purified by crystallization from EtOH. Obtained in 86% yield as a white solid. M.p. 142-144 °C. TLC (7:3 *n*-hexane-EtOAc, Rf: 0.66). One set of signals observed in NMR experiments. ¹H-NMR (CDCl₃), δ: 1.33 (s, 9H), 1.41-1.47 (m, 4H), 1.59-1.61 (m, 1H), 1.76-1.81 (m, 1H), 1.86-1.91 (m, 4H), 2.20 (s, 3H), 2.53-2.58 (m, 1H), 3.04-3.08 (m, 2H), 3.10-3.14 (m, 2H), 7.23-7.27 (m, 4H), 7.35 (d, J = 6.7 Hz, 2H), 7.68 (d, J = 6.9 Hz, 2H), 8.55 (bs, 1H). ¹³C-NMR (CDCl₃), δ: 12.4, 21.4, 26.1, 26.8, 34.3, 34.7, 30.1, 44.3, 125.3, 126.1, 126.9, 128.1, 135.4, 138.2, 146.7, 148.8, 149.6, 175.1. Anal. Calcd for C₂₇H₃₆N₂O: C, 80.15; H, 8.97; N, 6.92. Found: C, 79.93; H, 9.15; N, 6.97. MS [ESI, m/z]: 405.2 [M+H].

S.1.1.27 *N'*-(1-(4-Cyclohexylphenyl)ethylidene)-3-phenylpropanehydrazide (**32c**)

Purified by crystallization from EtOH. Obtained in 90% yield as a white solid. M.p. 119-121 °C. TLC (6:4 *n*-hexane-EtOAc, Rf: 0.61). One set of signals observed in NMR experiments. ¹H-NMR (DMSO-d₆), δ: 1.18-1.27 (m, 2H), 1.31-1.44 (m, 6H), 1.67-1.73 (m, 4H), 1.74-1.81 (m, 8H), 2.20 (s, 6H), 2.46-2.48 (m, 2H), 2.62-2.66 (m, 2H), 2.88-2.93 (m, 4H), 2.94-2.98 (m, 2H), 7.16-7.21 (m, 2H), 7.22-7.31 (m, 12H), 7.65 (d, J = 8.2 Hz, 2H), 7.68 (d, J = 8.2 Hz, 2H), 10.27 (bs, 1H), 10.43 (bs, 1H). ¹³C-NMR (DMSO-d₆), δ: 13.4, 25.5, 26.3, 30.0, 30.8, 33.7, 34.3, 35.5, 43.4, 125.8, 125.9, 126.2, 126.5, 126.6, 128.2, 128.3, 141.1, 147.1, 148.7, 174.2. Anal. Calcd for C₂₃H₂₈N₂O: C, 79.27; H, 8.10; N, 8.04. Found: C, 79.41; H, 8.02; N, 7.91. MS [ESI, m/z]: 349.1 [M+H].

S.1.2 General method for the preparation of amides **25**, **26**

A mixture of the appropriate acid **9a** or **9c** (1 eq) and TBTU (1.2 eq.) was suspended in anhydrous THF (5 ml · mmol/eq.) at r.t. under a N₂ atmosphere. DiPEA (2.5 eq.) was then added to the reaction, followed by the appropriate benzyl amine (1 eq.). The reaction was stirred at r.t. for 4-8 hours (monitored by T.L.C.), then diluted with EtOAc (50 ml · mmol/eq.). The organic phase was washed with 0.5M aq. citric acid solution (2x 30 ml · mmol/eq), sat. aq. NaHCO₃ solution (2x 30 ml · mmol/eq), and finally with brine (30 ml · mmol/eq). The organic layer was dried over Na₂SO₄ concentrated under vacuum. The solid obtained was purified by crystallization or flash column chromatography.

S.1.2.1 (E)-3-(4-(*tert*-Butyl)phenyl)-*N*-(4-(trifluoromethyl)benzyl)acrylamide (**25a**)

Purified by crystallisation from MeOH. Obtained in 67% yield as a white solid. M.p. 150-154 °C. TLC (5:5 *n*-hexane-EtOAc, Rf: 0.72). ¹H-NMR (CDCl₃), δ: 1.34 (s, 9H), 4.64 (d, J= 5.9 Hz, 2H), 6.15 (t, J= 5.9 Hz, 1H), 6.44 (d, J= 15.5 Hz, 1H), 7.40 (d, J= 8.4 Hz, 2H), 7.44-7.47 (m, 4H), 7.61 (d, J= 8.1 Hz, 2H), 7.69 (d, J= 15.5 Hz, 1H). ¹³C-NMR (CDCl₃), δ: 31.1, 34.8, 43.2, 119.1, 125.5, 125.7, 126.8, 127.7, 127.9, 129.6, 129.9, 131.8, 141.8, 142.4, 166.2. Anal. Calcd for C₂₁H₂₂F₃NO: C, 69.79; H, 6.14; N, 3.88. Found: C, 69.60; H, 5.97; N, 4.03. MS [ESI, m/z]: 384.1 [M+Na].

S.1.2.2 *N*-(4-(Trifluoromethyl)benzyl)cinnamamide (**25c**)

Purified by crystallisation from MeOH. Obtained in 86% yield as a white solid. M.p. 130-132 °C. TLC (5:5 *n*-hexane-EtOAc, Rf: 0.69). ¹H-NMR (CDCl₃), δ: 4.63 (d, J= 5.9 Hz, 2H), 6.28 (t, J= 5.9 Hz, 1H), 6.48 (d, J= 15.6 Hz, 1H), 7.36-7.38 (m, 3H), 7.44 (d, J= 8.1 Hz, 2H), 7.48-7.51 (m, 2H), 7.58 (d, J= 8.1 Hz), 7.70 (d, J= 15.6 Hz, 1H). ¹³C-NMR (CDCl₃), δ: 43.2, 120.0, 123.0, 125.5, 125.6, 125.7, 127.9, 128.8, 129.9, 134.6, 141.9, 142.4, 166.0. Anal. Calcd for C₁₇H₁₄F₃NO: C, 66.88; H, 4.62; N, 4.59. Found: C, 67.02; H, 4.55; N, 4.37. MS [ESI, m/z]: 306.1 [M+H].

S.1.2.3 (E)-*N*-([1,1'-Biphenyl]-4-ylmethyl)-3-(4-(*tert*-butyl)phenyl)acrylamide (**26a**)

Purified by crystallisation from MeOH. Obtained in 94% yield as a white solid. M.p. 140-144 °C. TLC (5:5 *n*-hexane-EtOAc, Rf: 0.79). ¹H-NMR (CDCl₃), δ: 1.35 (s, 9H), 4.64 (d, J= 5.7 Hz, 2H), 5.97 (t, J= 5.7 Hz, 1H), 6.42 (d, J= 15.5 Hz, 1H), 7.37 (m, 1H), 7.40-7.45 (m, 4H), 7.45-7.48 (m, 4H), 7.58-7.61 (m, 4H), 7.70 (d, J= 15.5 Hz, 1H). ¹³C-NMR (CDCl₃), δ: 31.1, 35.2, 43.5, 119.5, 125.8, 127.1, 127.3, 127.5, 127.6, 128.4, 128.8, 132.0, 137.3, 140.6, 140.7, 141.3, 153.2, 166.0. Anal. Calcd for C₂₆H₂₇NO: C, 84.51; H, 7.37; N, 3.79. Found: C, 84.77; H, 7.41; N, 3.65. MS [ESI, m/z]: 392.2 [M+Na].

S.1.2.4 *N*-([1,1'-Biphenyl]-4-ylmethyl)cinnamamide (**26c**)

Purified by crystallisation from MeOH. Obtained in 83% yield as a white solid. M.p. 162-166 °C. TLC (6:4 *n*-hexane-EtOAc, Rf: 0.48). ¹H-NMR (CDCl₃), δ: 4.65 (d, J= 5.8 Hz, 2H), 5.96 (t, J= 5.8 Hz, 1H), 7.37-7.40 (m, 4H), 7.43 (d, J= 8.2 Hz, 2H), 7.44-7.48 (m, 2H), 7.45 (d, J= 15.6 Hz, 1H), 7.52-7.54 (m, 2H), 7.59-7.61 (m, 4H), 7.72 (d, J= 15.6 Hz, 1H). ¹³C-NMR (CDCl₃), δ: 43.6, 120.3, 127.1, 127.3, 127.5, 127.8, 128.4, 128.8, 128.9, 129.7, 134.8, 137.2, 140.6, 140.7, 141.5, 165.7. Anal. Calcd for C₂₂H₁₉NO: C, 84.31; H, 6.11; N, 4.47. Found: C, 84.15; H, 5.87; N, 4.51. MS [ESI, m/z]: 314.2 [M+H].

S.2 Molecular Modelling

All molecular modeling studies were performed on a MacPro dual 2.66 GHz Xeon running Ubuntu 14.04. CHIKV nsP2 protease crystal structure was downloaded from the PDB data bank (<http://www.rcsb.org/>; PDB code 3TRK). Hydrogen atoms were added to the protein, using the Protonate 3D routine of the Molecular Operating Environment (MOE2015.10).^{S3} Ligand structures were built with MOE and minimized using the MMFF94x force field until a RMSD gradient of 0.05 kcal mol⁻¹ was reached. The Maestro LigPrep tool^{S4} was used to prepare the ligands using the default settings, whereas the protein was prepared using the preparation wizard tool.^{S5} The docking simulations were performed using Maestro Glide SP using the default parameters.^{S6}

S.3 Virus cell-based CPE reduction assay

Chikungunya virus, Indian Ocean strain 889, isolated in 2006, was cultured on African green monkey kidney (Vero) cells (ATCC CCL-81) in minimum essential medium MEM Rega3 (Invitrogen, Belgium) supplemented with 10% Foetal Bovine Serum (FBS; Integro, The Netherlands), 1% L-glutamine and 1% sodium bicarbonate (Invitrogen). Antiviral assays were performed in MEM Rega-3 medium supplemented with 2% FBS.

Vero cells were seeded in 96-well tissue culture plates (Becton Dickinson Falcon 96-Well Cell Culture Plate) at a density of 2.5×10^4 cells/well in 100 μ l assay medium and were allowed to adhere overnight in an incubator (37 °C, 5% CO₂, 95-99% RH). Next, a compound dilution series was added after which the cultures were infected with 0.01 MOI of CHIKV 899 in 100 μ l assay medium and returned to the incubator. Each assay was performed in triplicate in the same test and assays were repeated independently. On day 5 post-infection (p.i.), the cell viability in each assay well was measured using the MTS/PMS method as described by the manufacturer (Promega, The Netherlands). Chloroquine was included in the assay as a reference compound.^{S7} The 50% effective concentration (EC₅₀) is defined as the compound concentration that is required to inhibit virus-induced cytopathogenic effect (CPE) by 50% and was determined using logarithmic interpolation employing a custom-designed database-coupled interface (Accelrys, United Kingdom). The anti-metabolic effect of the compounds was evaluated in uninfected, compound-treated cells, also by means of the MTS/PMS method. The 50% cytostatic/cytotoxic concentration (CC₅₀) is defined to be the concentration of compound that reduces the overall metabolic activity of the uninfected, compound-treated cells by 50%, and was calculated using logarithmic interpolation. All assay wells were checked microscopically for minor signs of virus-induced CPE or alterations of the cell or monolayer morphology.

References

- S1** Bassetto, M.; De Burghgrave, T.; Delang, L.; Massarotti, A.; Coluccia, A.; Zonta, N.; Gatti, V.; Colombano, G.; Sorba, G.; Silvestri, R.; Tron, G.C.; Neyts, J.; Leyssen, P.; Brancale, A. Computer-aided identification, design and synthesis of a novel series of compounds with selective antiviral activity against chikungunya virus. *Antiviral Res.* **2013**, 98, 12-18.
- S2** Cheung, S.Y.; Chow, H.F.; Ngai, T.; Wei, X. Synthesis of organometallic poly(dendrimer)s by macromonomer polymerization: effect of dendrimer size and structural rigidity on the polymerization efficiency. *Chem. Eur. J.* **2009**, 15, 2278-2288.
- S3** Molecular Operating Environment (MOE 2015.10); Chemical Computing Group, Inc.: Montreal, Quebec, Canada; URL <<http://www.chemcomp.com>>; **2015**.
- S4** Schrödinger Release 2017-1: LigPrep, New York, NY: Schrödinger, LLC; 2017.
- S5** Schrödinger Release 2017-1: Schrödinger Suite 2017-1 Protein Preparation Wizard; Epik, New York, NY: Schrödinger, LLC; 2017; Impact, New York, NY: Schrödinger, LLC; 2017; Prime, New York, NY: Schrödinger, LLC; 2017.
- S6** Schrödinger Release 2017-1: Glide, Schrödinger, LLC, New York, NY, 2017.
- S7** Khan, M.; Santosh, S.R.; Tiwari, M.; Lakshmana Rao, P.V.; Parida, M. Assessment of in vitro prophylactic and therapeutic efficacy of chloroquine against chikungunya virus in vero cells. *J. Med. Virol.* **2010**, 82, 817–824.